

A young hierarchical triple system harbouring a candidate debris disc[★]

N. R. Deacon,[†] J. E. Schlieder, J. Olofsson, K. G. Johnston and Th. Henning

Max Planck Institute for Astronomy, Königstuhl 17, D-69117 Heidelberg, Germany

Accepted 2013 June 11. Received 2013 June 10; in original form 2013 March 5

ABSTRACT

We report the detection of a wide young hierarchical triple system where the primary has a candidate debris disc. The primary, TYC 5241-986-1 A, is a known Tycho star which we classify as a late-K star with emission in the X-ray, near- and far-ultraviolet (UV) and H α suggestive of youth. Its proper motion, photometric distance (65–105 pc) and radial velocity lead us to associate the system with the broadly defined Local Association of young stars but not specifically with any young moving group. The presence of weak lithium absorption and X-ray and calcium H and K emission support an age in the 20 to \sim 125 Myr range. The secondary is a pair of M4.5 \pm 0.5 dwarfs with near- and far-UV and H α emission separated by approximately 1 arcsec (\sim 65–105 au projected separation) which lie of 145 arcsec (9200–15200 au) from the primary. The primary has a *Wide-field Infrared Survey Explorer* (WISE) 22 μ m excess and follow-up *Herschel* observations also detect an excess at 70 μ m. The excess emissions are indicative of a 100–175 K debris disc. We also explore the possibility that this excess could be due to a coincident background galaxy and conclude that this is unlikely. Debris discs are extremely rare around stars older than 15 Myr, hence if the excess is caused by a disc this is an extremely novel system.

Key words: surveys – binaries: visual – circumstellar material – stars: late-type – stars: pre-main-sequence.

1 INTRODUCTION

Since the late 1990s, several comoving groups of young stars have been identified in the solar neighbourhood (Zuckerman & Song 2004). These include the $<$ 20 Myr old β Pic moving group and TW Hydrae Association (TWA), the \sim 30 Myr Columba, Carina and Tucana–Horologium associations – which Torres et al. (2008) group together as the Great Austral Young Association (GAYA) – and the AB Dor moving group which may share its origins with the Pleiades (Barenfeld et al. 2013). These sit within a more general Local Association of stars younger than or equal to approximately Pleiades age (125 Myr; Stauffer, Schultz & Kirkpatrick 1998). As well as providing targets for direct-imaging studies of young extrasolar planets, these kinematic groups represent possible remnants of low-mass star formation events (Mamajek & Feigelson 2001). As such they are ideal targets to identify variations in the star formation process caused by environmental dependence. Theoretical models (Delgado-Donate et al. 2004; Kouwenhoven et al. 2010; Kaczmarek, Olczak & Pfalzner 2011; Reipurth & Mikkola 2012) have suggested that dynamical interactions within a forming cluster can alter the

population of binary stars. Evidence for such processing of binaries with separations $<$ 1000 au has recently been published by King et al. (2013). Hence any deviation in the wide ($>$ 1000 au) binary population of such groups when compared to the field will lead to constraints on the effect of formation environment dynamics on multiple systems. A number of wide multiple systems have been identified in young moving groups (Torres et al. 2008) including a number of recently identified hierarchical multiples (Shkolnik et al. 2012). However, there has been no systematic study of the widest binaries in these associations.

Debris discs around stars are collections of dust radiating in the mid-infrared to submillimetre. For \sim 10 Myr old discs, this dust could be the residuals of the steady state evolution of a protoplanetary disc (Wyatt 2008), the dust in older discs is thought to be accompanied by a population of planetesimals and is to be replenished by collisions between such objects (Backman & Paresce 1993). These planetesimals are the remnant of planet formation processes much like our own Solar system’s asteroid and Kuiper belts. An observational connection between debris discs and planet formation has been identified by Wyatt et al. (2012). They find evidence that stars with debris discs are more likely to host low-mass extrasolar planets.

While debris discs are commonly detected around stars of spectral types A to early-K (Su et al. 2006; Trilling et al. 2008; Moór et al. 2011), their detection is substantially less common in late-K or M dwarfs older than \sim 20 Myr. Currently only two resolved debris

[★]Based on observations collected at the German–Spanish Astronomical Center, Calar Alto, jointly operated by the Max-Planck-Institut für Astronomie Heidelberg and the Instituto de Astrofísica de Andalucía (CSIC).

[†]E-mail: deacon@mpia.de

discs are known around M dwarfs, around the M1 β Pic member AU Mic (Kalas, Liu & Matthews 2004) and around the field age M5 GJ 581 (Lestrade et al. 2012). In younger (<20 Myr) moving groups there are candidate debris discs with mid-infrared excesses around late-K and M stars such as β Pic members AT Mic (Plavchan et al. 2009) and GJ 182 (Liu et al. 2004) and three TW Hydrae members: TWA 3, TWA 7 (Low et al. 2005) and TWA 4 (Skinner, Barlow & Justtanont 1992). However, the number of observed late-type star (K5 or later) debris discs drops off with age. Simon et al. (2012) find no *Wide-field Infrared Survey Explorer* (*WISE*) excess suggestive of a disc in low-mass members of Tucana–Horologium or AB Doradus, while Avenhaus, Schmid & Meyer (2012) failed to identify *WISE* excesses caused by candidate discs in any of the 103 field M dwarfs they studied. Fujiwara et al. (2013) studied 191 K dwarfs and 19 M dwarfs with photospheres detectable with *Akari* 18 μm data and succeeded only in recovering TWA 4. However, Heng & Malik (2013) suggest that is due to the *WISE* satellite probing relatively small radii around late-type stars at which dust is unlikely to survive for very long. Currie et al. (2008) use *Spitzer* observations of the h and χ Persei clusters to claim that 24 μm emission from debris discs peaks around 10–15 Myr before falling off. At longer wavelengths, Donaldson et al. (2012) studied 6 K and M members of Tucana–Horologium with *Herschel* and found no excesses. Smith et al. (2006) find a 70 μm excess around the M2 dwarf HD 95650 which King et al. (2003) list as kinematic and possible photometric member of the ~ 500 Myr old Ursa Majoris moving group as well as the K5 dwarf BD +21°2486. Recently Eiroa et al. (2013) identified a cold, resolved disc around the late-K star HIP 49908. In the ~ 40 Myr old cluster NGC 2547, Forbrich et al. (2008) find 11 M dwarfs with 24 μm excess. Lestrade et al. (2009) use these observations to derive a disc fraction of 4.9 ± 1.8 per cent, however, Forbrich et al. (2008) state that their sample is not complete for M dwarfs and that it is possible that their debris disc fraction may be higher than for higher mass stars. Lestrade et al. (2006) find a cold debris disc in the submillimetre around the ~ 200 Myr star GJ 842.2. This combined with their observations of their entire sample lead them to measure cold disc fractions of $5.3^{+10.5}_{-5.0}$ per cent for M dwarfs in the 20–200 Myr age range and <10 per cent for older field objects. In summary, candidate debris discs around late-K and M dwarfs are rare after 20 Myr. However, it is unclear if this is a true dearth or due to biases in the current searches. Lestrade et al. (2009) outline a number of possible mechanisms as to why M dwarf discs are likely to disperse faster or be less observable than those around higher mass stars.

Schlieder, Lépine & Simon (2012a) identified a list of Northern hemisphere candidate members of the β Pic and AB Dor moving groups based on their proper motions, photometry and ultraviolet (UV) and X-ray emission. We took a companion list of candidate Southern hemisphere members of moving groups (Schlieder, in preparation) and searched for companion objects in the SuperCOSMOS Sky Survey. In this paper, we report the discovery of a wide multiple system which has one component that harbours a possible debris disc.

2 IDENTIFICATION OF THE SYSTEM

The input list in our search for wide companions consisted of 191 candidate Southern hemisphere moving group members. These were selected using the same selection criteria as Schlieder et al. (2012a) with objects initially identified as (1) having a proper motion vector aligned to within 10° of the local projection of the

space velocity of the moving group, (2) colour–magnitude diagram placement consistent with other moving group members when using a kinematic distance estimate that assumes group membership, (3) having a $(V - K_s) \geq 3.2$ (suggesting that they are M dwarfs) and (4) having emission in UV ($\log(F_{\text{NUV}}/F_{K_s}) \geq 4.1$ or $\log(F_{\text{FUV}}/F_{K_s}) \geq 5.1$) or X-ray ($\log(F_X/F_{K_s}) \geq 2.6$) indicative of youth.¹ The target primary stars come from a southern extension to Lépine & Shara (2005) (Lépine, private communication). The stars are candidate members of TWA, β Pic, Tucana–Horologium and AB Dor. However as many young associations have similar kinematics and ages, these objects may also be candidate members of other moving groups. We ran an initial search on the SuperCOSMOS Science Archive within 5 arcmin of each candidate star and identified objects with proper motion measurements more significant than 5σ and which met the *Galaxy Evolution Explorer* (*GALEX*; Martin et al. 2005) far- and/or near-UV activity cuts set out by Schlieder et al. (2012a). We identified 2652 objects within 5 arcmin of our targets which passed our proper motion significance cuts, 220 of these passed our UV cut. We then plotted the significance of the proper motion difference² between the SuperCOSMOS proper motions of both objects against their projected separations. This is shown in Fig. 3. Note two objects stand out, one is TYC 7443-1102-1 B, a known wide companion to a β Pic member from Lépine & Simon (2009). The other obvious outlier is TYC 5241-986-1, a star in the Tycho catalogue. It appears to be a 145 arcsec companion to PM I22595–0704, a candidate member of the Tucana–Horologium moving group based on its proper motion and colour–magnitude diagram placement (Schlieder et al., in preparation). We found this star had emission suggestive of activity (and hence youth) in the X-ray region from *ROSAT* (Voges et al. 2000) and in the near- and far-UV from *GALEX* (Martin et al. 2005). TYC 5241-986-1 was not in our input list of candidate moving group members as although it has sufficient X-ray and UV emission to pass those cuts, it had a $V - K_s$ colour that was bluer than the cut defined by Schlieder et al. (2012a). This $V - K_s \geq 3.2$ cut was due to their search being specifically for M dwarf members, our search includes no such cut and hence can include earlier type companions. Images of TYC 5241-986-1 in multiple filters are shown in Fig. 1 with similar plots for PM I22595–0704 in Fig. 2. Inspecting Sloan Digital Sky Survey (SDSS; Ahn et al. 2012) images of PM I22595–0704 revealed that it is itself a close binary system with a flux ratio close to unity. For more details on both components, see Table 1. As TYC 5241-986-1 is a previously catalogued object, we will refer to the entire system as TYC 5241-986-1 A and TYC 5241-986-1 B/C.

After extracting the *WISE* (Wright et al. 2010; Cutri et al. 2012) photometry for TYC 5241-986-1 A, we noted it had a particularly striking $W3 - W4$ colour of 1.64 mag. This combined with it being colour neutral in colours involving $W1$, $W2$ and $W3$ makes it similar to the debris disc star HD 191089 (Mannings & Barlow 1998). This along with its possible membership of a young moving group with an age of 30 Myr (Zuckerman & Song 2004) makes it an interesting target for further characterization.

¹ Note that these are only candidate members of a particular moving group. Follow-up observations are required for each to determine the full 3D kinematics and to measure youth indicators before their membership can be confirmed.

² The quadrature sum of the proper motion difference in each axis divided by the total error in that axis.

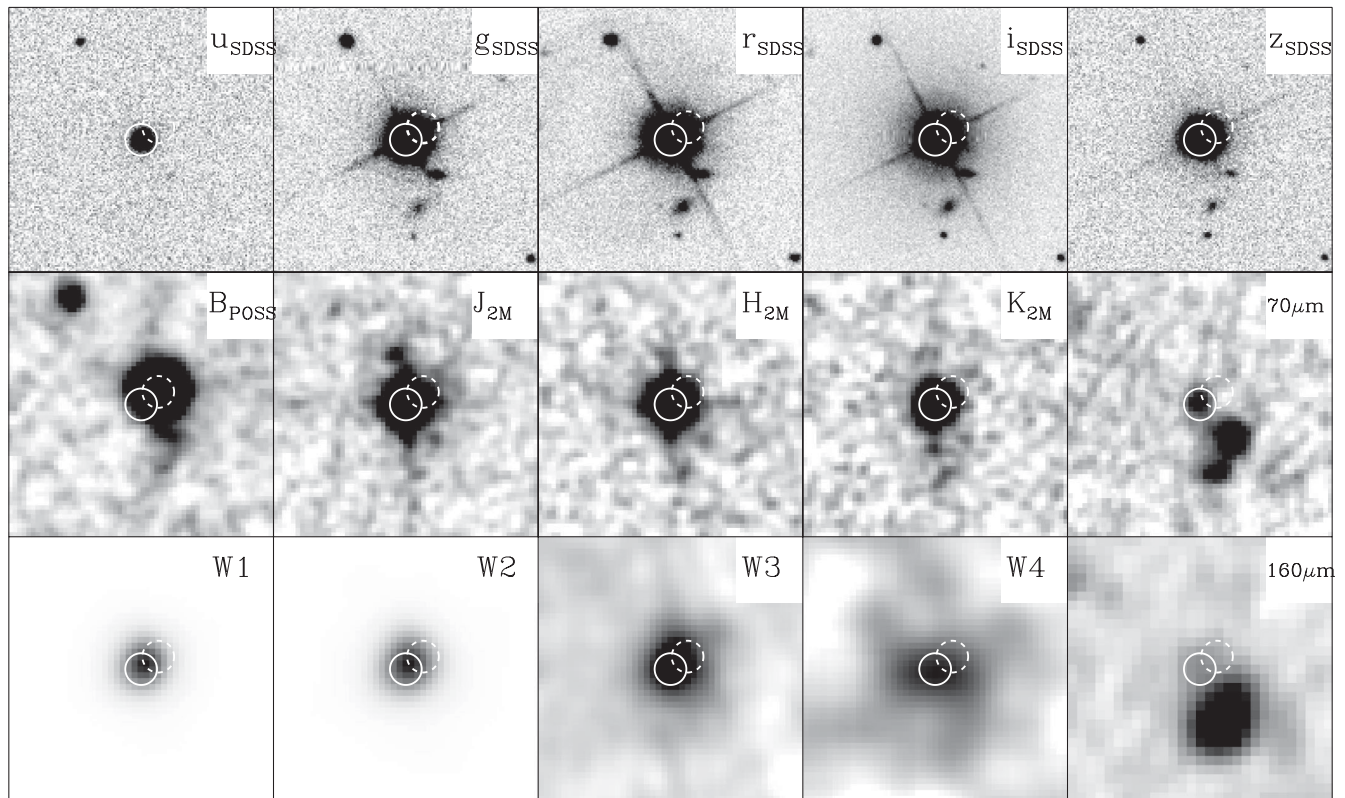


Figure 1. Multiband images of TYC 5241-986-1 A. The image size is 1 arcmin with the solid circle centred on the 2013.0 position and the dashed circle on the POSS-I *B* position. Note the clear detection in the *Herschel* 70 μm band. While this is slightly offset from the position of the star, the positional difference of 2.6 arcsec is well comparable to the *Herschel* astrometric accuracy of 2.5 arcsec. Note also the two faint spiral galaxies in the SDSS images, these have strong emission in the *Herschel* 70 and 160 μm bands. See Section 4.4 for more discussion on the possibility that these are part of a background galaxy cluster.

2.1 Companionship

There are several checks we can apply to infer if these objects are a likely pair. First, Dupuy & Liu (2012) asserted that objects with $\delta\mu/\mu > 0.2$ were unlikely to be a true pair. This system has a fractional proper motion difference of 0.07. Lépine & Bongiorno (2007) derived several metrics to judge if a pair was a true pair or a pairing with a background star with coincident proper motion. They produced a purely coincident population by offsetting the positions of their input list by angles of a few degrees to generate pairings with background stars. We applied the same method by shifting the RA coordinates of our input list by 2° and then following through the proper motion significance and UV cuts we applied to identify the star. The results are shown as grey dots in Fig. 3. Clearly our system lies well outside the coincident population. Lépine & Bongiorno (2007) also provide an inequality comparing the product of the proper motion and angular separation with the total proper motion of the system ($\Delta\mu \times \text{separation} < (\mu/0.15)^{3.8}$). This is based on the distribution of proper motions of all stars in their catalogue and is equal when an object has a 50 per cent chance of being a coincident pairing. Hence if an object passes the inequality, it is likely a companion. If we apply this to our system we find that it fails their condition with values of 0.88 and 0.138 for the two sides of the inequality. However, the right-hand side of the Lépine & Bongiorno (2007) inequality is derived from pairings of all stars in their proper motion catalogue. We know that our two stars have UV emission suggestive of youth and hence are only drawn from a young subset of stars in the sky. Hence we must correct the right-hand side of the inequality to take this lower surface density of

coincident pairings with young stars in to account. Only 220 of the 2652 objects which passed our proper motion significance cut had sufficient emission to pass our UV cut. If we adjust the value of $(\mu/0.15)^{3.8}$ by a factor of 2652/220, then our system satisfies the Lépine & Bongiorno (2007) inequality.

3 CHARACTERIZATION OF THE COMPONENTS

3.1 TYC 5241-986-1 A

We obtained $R = 48\,000$ spectroscopic observations of TYC 5241-986-1 A using Fiber-fed Extended Range Optical Spectrograph (FEROS; Kaufer et al. 1999) on the MPG/ESO 2.2-m telescope in La Silla, Chile, on 2012 July 6 (UT). Three integrations of 500 s were used. The data were reduced using standard ESO-MIDAS FEROS packages and the normalized spectrum was cross-correlated over a number of orders with a suite of late-type templates from Prato et al. (2002) which have subsequently been observed using FEROS with the same set-up. This produced a radial velocity measurement of $-6.7 \pm 0.1 \text{ km s}^{-1}$ fitting K5 and M0 templates well. However, when we examined the star's $H\alpha$ profile, we were surprised to find two peaks above the continuum (see Fig. 4). Other prominent features in the spectrum did not appear to be double lines. To help understand the cause of this we re-observed the target using the same set-up on 2012 August 18 (UT). This time the $H\alpha$ profile appears as two emission features either side of the expected wavelength with absorption in between. Such self-absorption of $H\alpha$ emission is

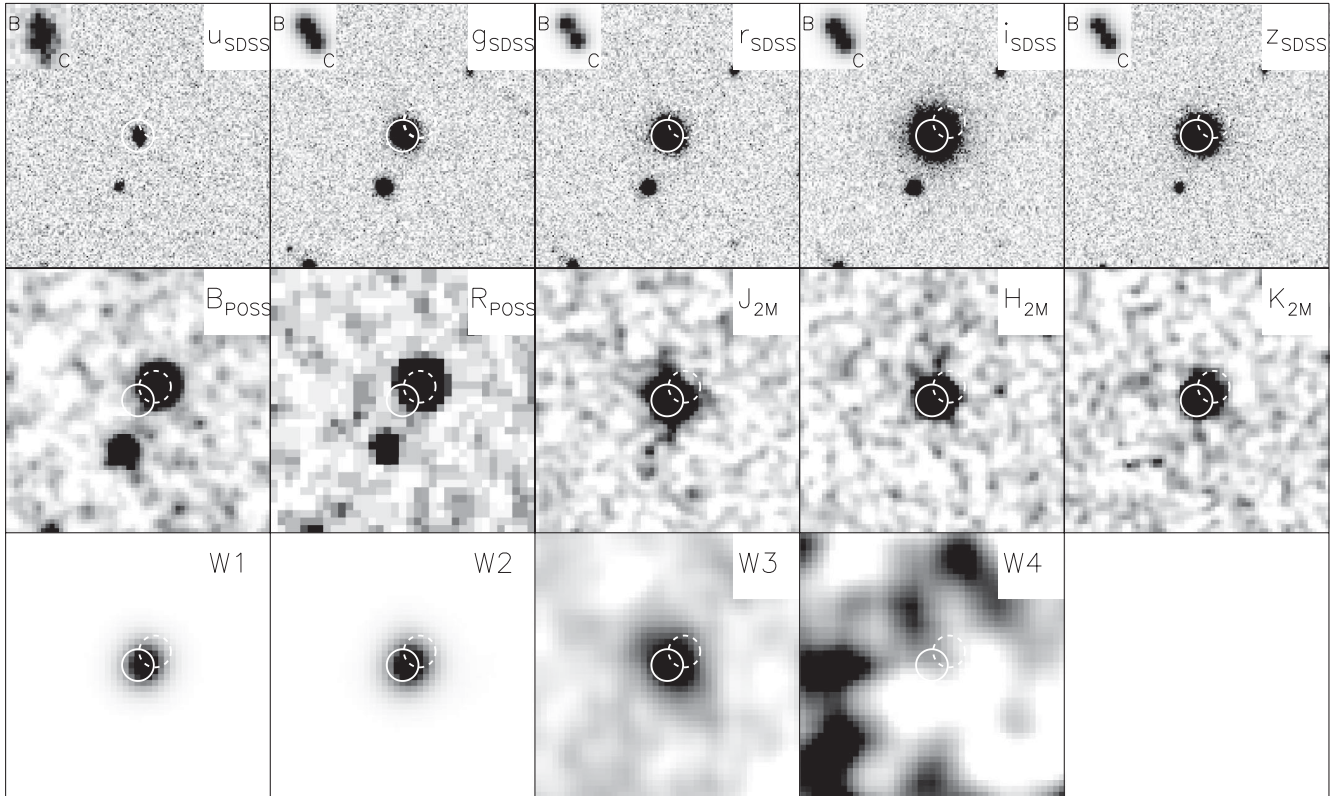


Figure 2. Multiband images of TYC 5241-986-1 B/C. The image size is 1 arcmin with the inset images 5 arcsec across. In the SDSS inset images it can clearly be seen that the object is a binary with a separation of 1–2 arcsec. Comparing with the POSS-I images from the 1950s it is clear that the two objects have moved with a common proper motion as there is no non-moving background star situated at the 2013.0 position (solid circle). The dotted circle marks the POSS-I *B* position. Note also that the two components of this object appear to have near, equal flux throughout the SDSS bands.

commonly seen in active M dwarfs (Worden, Schneeberger & Giampapa 1981; Houdebine, Doyle & Kosciielecki 1995; Mauas 2000). The radial velocity measurement for this second spectrum was $-6.7 \pm 0.1 \text{ km s}^{-1}$. In addition to $H\alpha$, emission was also seen in $H\epsilon$, calcium H and K and the Ca II infrared triplet in both spectra. These indicate that this is an extremely active star. It is notable that the depth of the $H\alpha$ self-absorption and the height of the emission in other lines appear to be stronger in the second spectrum. Fig. 4 shows cut-outs for some of the regions with emission lines as well as the 6707.8 \AA lithium absorption feature. This is weak, measuring only $\sim 8 \text{ m\AA}$ in equivalent width averaged over our two spectra. As our spectrum is of such high resolution, there are hardly any regions of continuum to measure the noise from. Hence we use our two independent measurements from our two spectra finding a scatter on the measurements of approximately 4 m\AA . Mentuch et al. (2008) show lithium measurements for some late-K and early-M dwarfs in β Pic of a few tenths of an Angstrom. Tucana–Horologium shows a mixture of values from these types of stars, from a few tenths of an Angstrom to some measurements which are in the $40\text{--}50 \text{ m\AA}$ range, while AB Dor members in this spectral range show lithium equivalent widths mostly below 50 m\AA and often consistent with zero. Torres et al. (2008) indicate that a star of this colour ($V_c - I_c = 1.9 \text{ mag}$) is close to the lithium depletion boundary for the Pleiades. Given that we have a very weak lithium detection we find it unlikely that our object is substantially older than this cluster ($\sim 125 \text{ Myr}$; Stauffer et al. 1998). We can also infer our object is probably older than β Pic and may be older than Tucana–Horologium. While lithium depletion is not a simple monotonic

clock for stellar ages, the weak lithium absorption in this star indicates that it is more likely to be older than 20 Myr than substantially younger. We estimated the flux in the calcium H and K lines by measuring the equivalent width and converting to flux using the relations of Hall (1996). This yielded values of $\log R'_{\text{HK}} = -3.63$ and -3.8 for our first and second spectra, respectively. This is consistent with stars of a similar spectral type in the Pleiades (Soderblom & Mayor 1993; King et al. 2003), but inconsistent with members of Ursa Majoris (López-Santiago et al. 2010). The latter paper also studied a number of proposed members of AB Dor, these have values comparable with TYC 5241-986-1 A. Mamajek & Hillenbrand (2008) find that $\log R'_{\text{HK}}$ saturates at approximately the value we find for TYC 5241-986-1 A. Hence we cannot use this to set a lower age boundary. From these constraints, we can say that the TYC 5241-986-1 system is likely older than 20 Myr and younger than the 500 Myr old Ursa Majoris group. Its activity and lithium measurements match the members of AB Dor and the Pleiades well, indicating that it may be of similar age ($\sim 125 \text{ Myr}$) and unlikely to be significantly older.

We estimated the rotational velocity TYC 5241-986-1 A by comparing its spectrum to artificially broadened versions of our template spectra. This was done in steps of 2 km s^{-1} with a $v \sin i$ of 8 km s^{-1} giving the best correlation. We then calculated the maximum rotational period at 20 and 125 Myr by combining the rotational velocity with radii calculated from the Baraffe et al. (1998) models. This resulted in maximum rotational periods of $\sim 6 \text{ d}$ for an age of 30 Myr and $\sim 4 \text{ d}$ for 125 Myr . Eyer & Blake (2005) identified TYC 5241-986-1 A as a photometric variable with a period of 8 d . As this

Table 1. Details of the photometry and astrometry for the A and integrated B/C components of the TYC 5241-986-1 system.

	TYC 5241-986-1 A	TYC 5241-986-1 B/C (integrated)
Position (J2000)	22 ^h 59 ^m 34 ^s .99, −07°02′22″.7 ^a	22 ^h 59 ^m 34 ^s .84, −07°04′46″.7 ^a
Epoch	1998.841 ^a	1998.841 ^a
$\mu_\alpha \cos \delta$ (mas yr ^{−1})	69 ± 11 ^b	70 ± 9 ^b
μ_δ (mas yr ^{−1})	67.0 ± 3.8 ^c −57 ± 10 ^b −53.7 ± 3.5 ^c	−51 ± 9 ^b
B_J (mag)	12.33 ^b	16.17 ^b
B (mag)	12.78 ± 0.29 ^c	
V (mag)	11.59 ± 0.14 ^c	15.4 ^d
R (mag)	10.48 ^b	13.91 ^b
I_N (mag)	9.53 ^b	11.68 ^b
J (mag)	9.47 ± 0.03 ^a	11.01 ± 0.04 ^a
H (mag)	8.77 ± 0.05 ^a	10.38 ± 0.03 ^a
K_s (mag)	8.67 ± 0.02 ^a	10.13 ± 0.03 ^a
$W1$ (mag)	8.56 ± 0.03 ^e	9.84 ± 0.04 ^e
$W2$ (mag)	8.58 ± 0.02 ^e	9.65 ± 0.02 ^e
$W3$ (mag)	8.50 ± 0.05 ^e	9.36 ± 0.10 ^e
$W4$ (mag)	7.36 ± 0.18 ^e	>8.4 ^e
Herschel/PACS 70 μm (mJy)	7.1 ± 1.8	
$\log(f_X/f_{K_s})$	−1.93 ^f	Undetected ^f
$\log(f_{\text{NUV}}/f_{K_s})$	−3.45 ^{a, g}	−3.90 ^{a, g}
$\log(f_{\text{FUV}}/f_{K_s})$	−4.49 ^{a, g}	−4.03 ^{a, g}
Spectral type	Late-K ^h	M4.5 ± 0.5 ^h

Notes. Citation key: ^aSkrutskie et al. (2006); ^bHambly et al. (2001); ^cHøg et al. (2000); ^dLépine (private communication) calculated using photographic plates magnitudes and the method of Lépine & Shara (2005); ^eWright et al. (2010) and Cutri et al. (2012); ^fVoges et al. (2000); ^gMartin et al. (2005); ^hthis work.

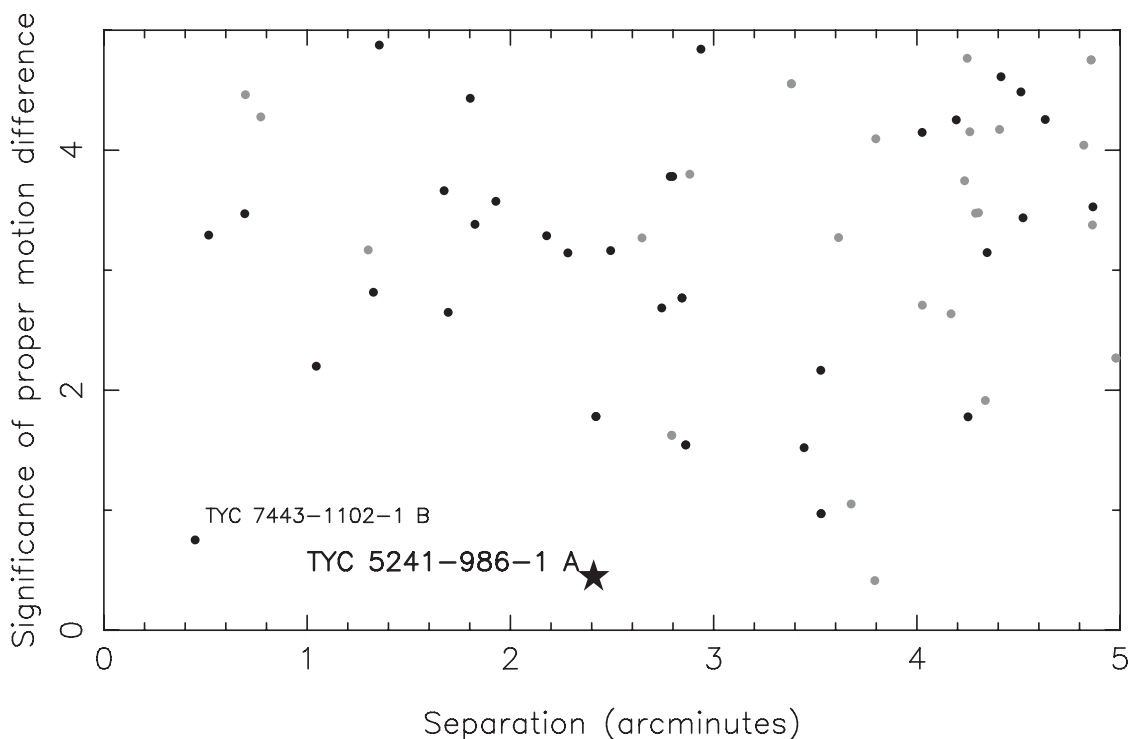


Figure 3. TYC 5241-986-1 A shown with other stars selected by the same proper motion and UV excess cuts (black points). The y-axis is the quadrature sum of the proper motion differences in each axis divided by the error on the proper motion measurement in that axis. The grey points show objects paired together using the offset method of Lépine & Bongiorno (2007), these should be random pairings. It appears that TYC 5241-986-1 A lies outside the coincident distribution. Note also our recovery of TYC 7443-1102-1 B (Lépine & Simon 2009) as a wide companion.

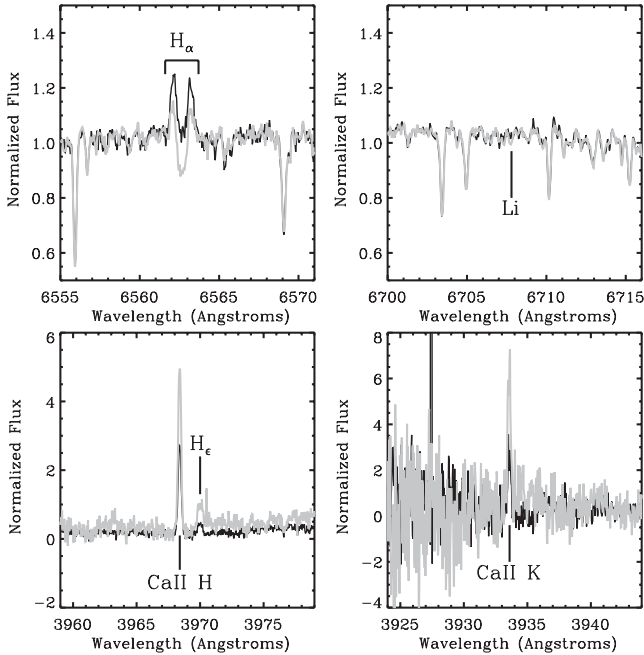


Figure 4. Portions of our FEROS spectrum for TYC 5241-986-1 A. The black line represents the spectrum taken on 2012 July 6 UT and the grey line the spectrum from 2012 August 28 UT. The star has emission in $H\alpha$, He and calcium H and K (all shown). The calcium K line lies at the blue end of a FEROS order and is thus in a noisy region of the spectrum. Additionally there is emission in the core of the three lines of the Ca II infrared triplet. We interpret the $H\alpha$ profile as emission with self-absorption. The 6707.8 Å lithium feature is extremely weak having an equivalent width of ~ 10 mÅ. In the first epoch spectrum this appears to be contaminated by a noise spike but is much clearer in the second epoch. Note the $H\alpha$ self-absorption and He and calcium H and K emission are all stronger in the second epoch.

is a measured photometric period we prefer this over our period determined from rotational velocity. Comparing with fig. 9 from Mamajek & Hillenbrand (2008) shows that for both ages, the star would fall on the slower rotator sequence for the Pleiades with a period too short to be consistent with the Hyades. This is another indicator that TYC 5241-986-1 A is unlikely to be significantly older than the Pleiades.

These constraints in addition to TYC 5241-986-1 A having significant UV excess (suggested by Shkolnik et al. 2011 as an indicator of an object being younger than 300 Myr) lead us to place an age range on this object of 20 to ~ 125 Myr.

As we do not have a flux calibrated single-order spectrum of TYC 5241-986-1 A, we used photometric methods to estimate the spectral type. Fitting our B , V , J , H , K_s , $W1$, $W2$ and $W3$ photometry to the model photospheres of Castelli & Kurucz (2003), we find a best-fitting temperature of 4200 K. We also compared the $V - K$ colour of the object to empirical relations from Kenyon & Hartmann (1995), finding 4380 ± 150 K. These two effective temperature values convert to spectral types of K6 and $K5 \pm 1$, respectively (using Kenyon & Hartmann 1995). To estimate the distance to TYC 5241-986-1 A, we compared the 2MASS photometry for the primary with models for populations with ages of 20 and 130 Myr from Baraffe et al. (1998). For the 20 Myr age and our two spectral type values, we find a distance range 85–105 pc. By the time our object has reached 125 Myr it is close to being on the main sequence. Hence for the 130 Myr models we derive distances of approximately

65 pc. As these are photometric distance estimates we note that this range is likely only accurate to approximately 20 per cent.

We estimated the X-ray luminosity of the star by combining its *ROSAT* (Voges et al. 2000) count rate and hardness ratio using the equation of Schmitt, Fleming & Giampapa (1995). This yielded a value of $L_x = 4.13 \pm 1.39 \times 10^{29}$ erg s^{-1} for our approximate 20 Myr distance of 95 pc and $L_x = 1.94 \pm 0.72 \times 10^{29}$ erg s^{-1} for 65 pc (our ~ 130 Myr distance). We then took the bolometric magnitude from the Baraffe et al. (1998) models and used this to calculate R_x . For the 20 Myr case we derived $\log R_x = -3.4$ and -3.3 for the ~ 125 Myr. Again this is in the range of activity values Mamajek & Hillenbrand (2008) find to be too saturated to be a useful age indicator. All we can say from this value is that it is consistent with our previous age range of 20 to ~ 125 Myr.

3.2 TYC 5241-986-1 B/C

Spectroscopic observations of TYC 5241-986-1 B/C were obtained with the Calar Alto Faint Object Spectrograph (CAFOS) instrument on the Calar Alto 2.2-m telescope on 2012 December 8. Two 300-s exposures were obtained using the R-100 grating with the slit orientated to maximize the distance between the components in the resulting spectrum. An observation of the standard star BD+25°4655 was also obtained at similar airmass.

The resulting spectrum was heavily blended with a separation between the peak of each component of approximately 2 pixels. First, the images were bias subtracted and flat-fielded using standard IRAF routines. Then we fitted a low-order polynomial to each wavelength (excluding the two spectra) and subtracted this to remove background sky emission. The same procedure was followed for the standard star. We then employed the technique of Hynes (2002) to separate the blended spectra. The standard was used to define a model spectral profile. For each wavelength (i.e. row on the chip parallel to the slit), we fitted a Voigt function to the standard spectrum. This allowed us to derive how the parameters of the Voigt profile which describes the spectrum in the direction parallel to the slit vary with wavelength. The distributions of these parameters against wavelength were then smoothed by fitting a low-order polynomial to each. Then for each wavelength of the target star observation, we defined a model blended spectrum to be the sum of two Voigt profiles each with their own normalization and positional offset parallel to the slit. We then ran a Markov chain Monte Carlo analysis to find the best-fitting model parameters for both components at each wavelength. The spectrum for each component at each wavelength is the integral of the fitted Voigt profile for that component at that wavelength. The standard star was extracted using a similar technique but with only the normalization as a free parameter. The spectra were then wavelength calibrated using arc spectra and IRAF routines. Finally flux calibration was carried out by comparing the observed continuum flux of the standard with the measured values from Oke (1990). A low-order polynomial was fitted to the derived sensitivity function and this was used to correct the observations of the target. The final spectra of both components averaged over the two observations are shown in Fig. 5. It has an approximate noise of 3 counts based on regions of the pseudo-continuum.

We measured the spectral indices defined by Lépine, Rich & Shara (2003) and used their index to spectral-type relations to derive the spectral type of the B and C components. Table 2 shows the spectral index measurements along with the spectral type associated with each of these measurements. Based on these we derive

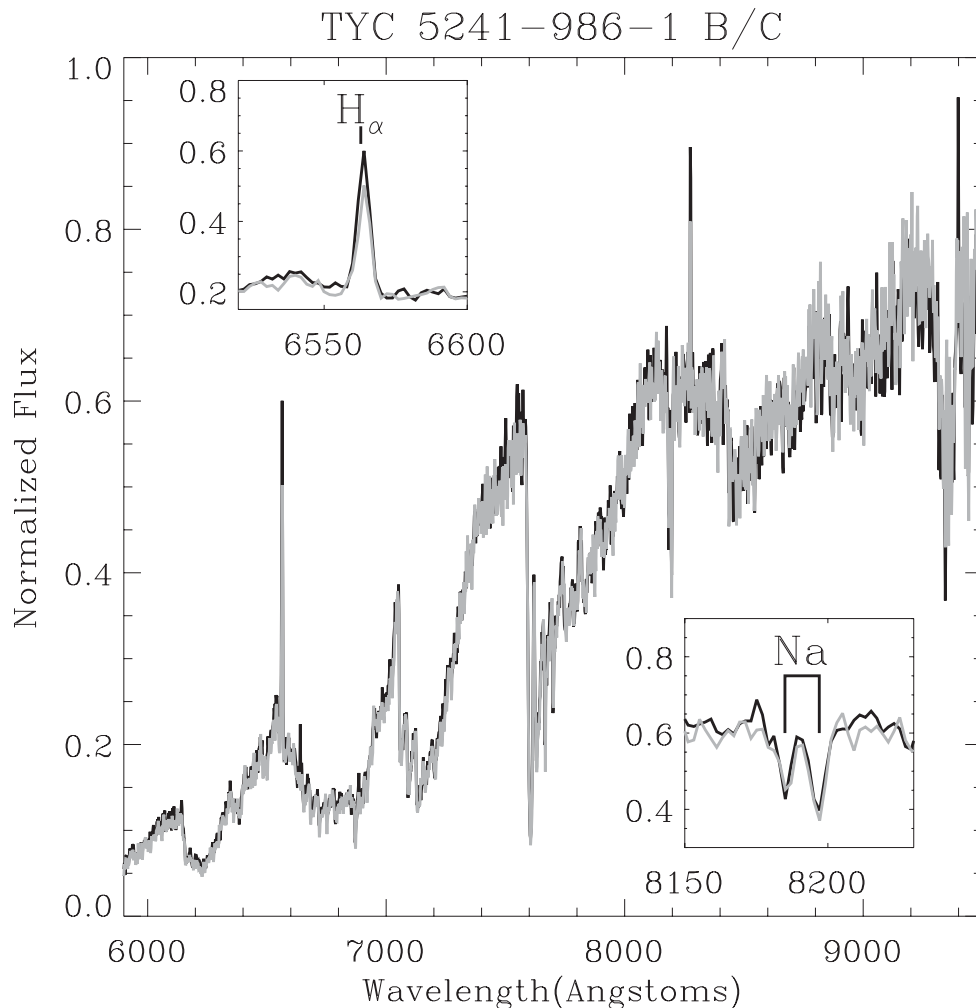


Figure 5. A plot of the spectra of both component B (black) and C (grey) of the TYC 5241-986-1 system. The insets show the H_{α} emission for both components and Sodium 8200 Å doublet. We type both components as active M4.5 dwarfs with an error of half a subtype (see text for details). The sodium doublet has equivalent widths of -3.5 ± 0.2 Å and 3.3 ± 0.3 Å for components B and C respectively. Comparing with measurements in Schlieder et al. (2012b) we conclude that the system is younger and has a lower gravity than typical field M dwarfs.

Table 2. The derived spectral indices for the B and C components of the system. The indices used here are defined by Lépine et al. (2003) and the spectral classifications in brackets are derived from the spectral-type relations for each index. Note we did not use the TiO6 feature due to significant telluric contamination.

Component	CaH2	CaH3	TiO5	TiO7	VO1	VO2	ColourM
B	0.378 (M4.0)	0.668 (M3.8)	0.365 (M4.2)	0.851 (M4.3)	0.881 (M5.3)	0.736 (M4.7)	2.793 (M4.9)
C	0.362 (M4.3)	0.632 (M4.4)	0.347 (M4.4)	0.841 (M4.4)	0.894 (M4.9)	0.711 (M4.9)	2.900 (M5.0)

a spectral type of $M4.5 \pm 0.5$ for both components. We also note that H_{α} is in emission for both components with equivalent widths of -9.9 ± 0.3 and -7.5 ± 0.2 Å for components B and C, respectively. However given the spectral type of both components, this does not set a strong constraint on their age. West et al. (2008) list a 1σ upper bound of 7.5 Gyr for an M5 star (the upper bound of our spectral type range). The equivalent widths of the gravity sensitive sodium 8200 Å doublet are -3.5 ± 0.2 and 3.3 ± 0.3 Å. These values are comparable to those of two proposed β Pic members of similar spectral type observed by Schlieder et al. (2012b). While this spectral feature cannot be used to set a strong age constraint, we note that these values make it likely that TYC 5241-986-1 B/C is younger than the typical population of field M dwarfs. In com-

mon with the primary these stars show UV excess, making them likely to be younger than 300 Myr. We followed a similar process to the primary when estimating the photometric distance to the secondary. One deviation was that we adjusted the 2MASS photometry by 0.75 mag to take into account that this approximately equal-flux binary is unresolved in this data set. From this we estimate the photometric distance to be in the range 65–90 pc. Taking into account the likely ~ 20 per cent error on this photometric distance, this is in agreement with the values of approximately 65 pc calculated for the primary at an age of 125 and the 20 Myr distance value of 85–105 pc. The similarity in photometric distances supports TYC 5241-986-1 B/C’s companionship with the primary.

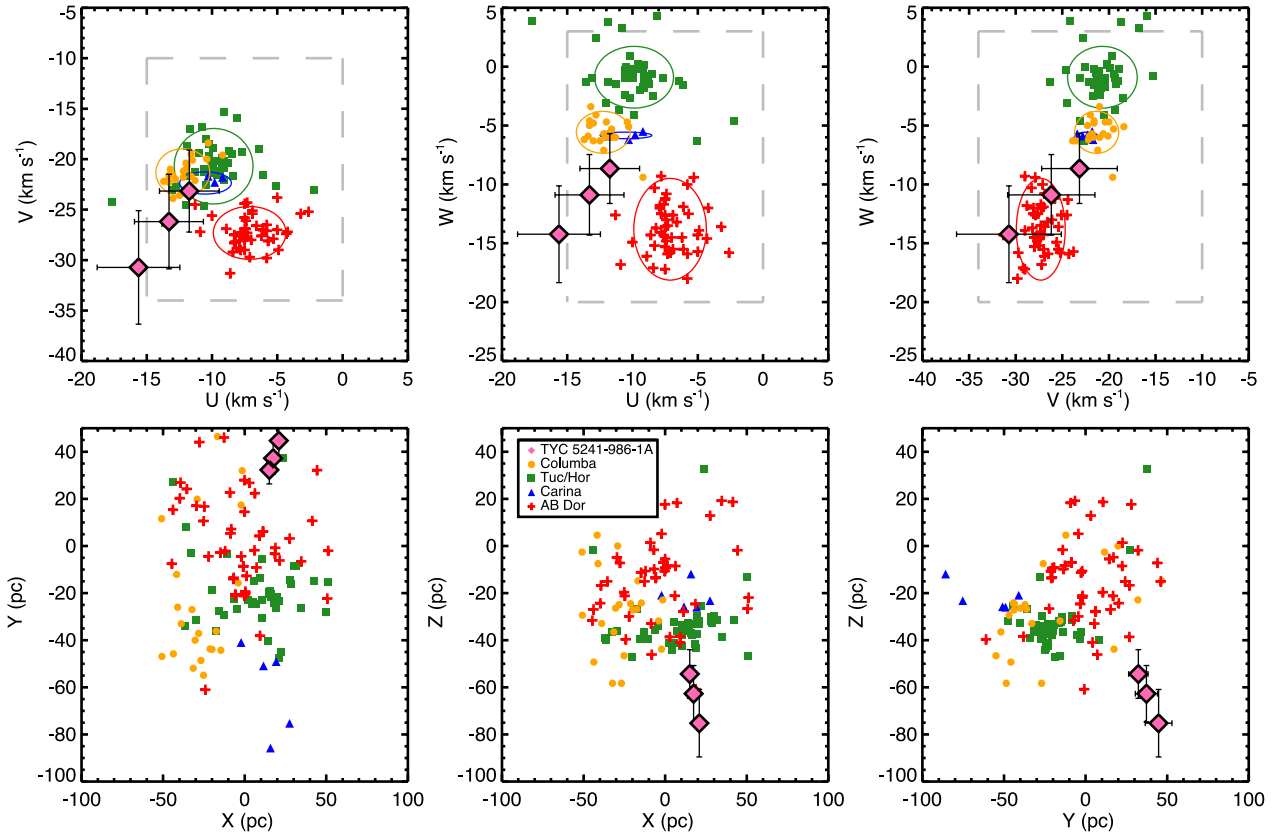


Figure 6. U , V , W , X , Y and Z projections for TYC 5241-986-1 A compared to several known young kinematic associations. TYC 5241-986-1 A is represented as a large diamond with associated error bars. The three data points, with smallest to largest errors, are for photometric distances/ages of 65 pc/130 Myr, 75 pc/80 Myr, 90 pc/20 Myr. The known group distribution symbol designations are given in the legend and the solid ellipses with like colours represent the 2σ errors on their average velocities. The dashed grey box represents the kinematic space occupied by nearby, young stars known as the Local Association. The top panels show that TYC 5241-986-1 A is only consistent with the 2σ error ellipse of the Columba and Carina associations in all three velocity projections, although at a photometric distance (65 pc) that corresponds to an age that is inconsistent with these associations. The bottom panels show that the galactic distances of TYC 5241-986-1 A are marginally consistent with the distributions of several associations. This is not a strong constraint on membership. Without a parallax measurement, we cannot suggest membership in any individual group and can only conclude that the TYC 5241-986-1 A system has kinematics and age consistent with the Local Association.

3.3 The architecture of the system

Comparing our approximate effective temperatures for all three components with the Baraffe et al. (1998) models we find masses of $\sim 0.7 M_{\odot}$ for the primary and $0.15\text{--}0.175 M_{\odot}$ for each of the secondary components. The two lower mass components of the system are separated by 145 arcsec from the primary, equating to a distance in the 9200–15200 au range. Comparing the total mass of the system and projected separation with the field binaries plotted in fig. 15 from Close et al. (2003), we find that this system is more loosely bound than any known system of similar mass within 25 pc. This indicates that this system may not survive to field age.

The fact that this is a hierarchical triple system is also interesting. Dhital et al. (2013) and references therein (i.e. Fischer & Marcy 1992; Reid & Gizis 1997) find that wide binaries have a far higher multiplicity fraction than field stars. This is taken as an indication that dynamical ejection of the low-mass pair played a role in forming the system.

3.4 Moving group membership

Since TYC 5241-986-1 B/C was originally selected as a candidate of the Tucana/Horologium association based on its proper motion and

photometry, we investigated its membership in several nearby kinematic associations. Given that we constrain the age of the system to be ~ 20 to ~ 125 Myr, we compare to five kinematic associations with comparable ages, the Tucana/Horologium, Columba and Carina associations (~ 30 Myr; Torres et al. 2008), the AB Doradus moving group (~ 125 Myr; Zuckerman & Song 2004; Torres et al. 2008; Barenfeld et al. 2013) and the Local Association ($\lesssim 125$ Myr; Zuckerman & Song 2004, and references therein). We followed the relations in Johnson & Soderblom (1987) to calculate the U , V , W galactic velocities and X , Y and Z galactic distances of TYC 5241-986-1 A from its published proper motion, measured radial velocity and photometric distance.³ Fig. 6 shows the 6D kinematic distributions of the five previously mentioned associations (Zuckerman & Song 2004; Malo et al. 2013) and TYC 5241-986-1 A. The top three panels are projections in U , V and W velocity, the bottom three are projections in X , Y and Z distance. We represent TYC 5241-986-1 A as a large diamond symbol with associated error bars. The known kinematic groups are represented by symbols defined in the

³ We define U and X positive towards the Galactic Centre, V and Y positive in the direction of solar motion around the Galaxy and W and Z positive towards the north Galactic pole.

figure legend with ellipses of matching colour in the U , V and W projections defining the 2σ error on the average velocities of the association (Malo et al. 2013). The dashed grey line represents the kinematic space of the Local Association of nearby, young stars (Zuckerman & Song 2004). TYC 5241-986-1 A is shown at three different estimates of the photometric distance which are indicative of different possible ages of the system, 65 pc–130 Myr, 75 pc–80 Myr, 90 pc–20 Myr. In the top panels, the only groups the Galactic velocities of TYC 5241-986-1 A are consistent with in all three projections are the Columba and Carina associations at a distance of 65 pc and the more general Local Association. However the 65 pc photometric distance corresponds to an age that is not consistent with the proposed ages of Columba and Carina. The bottom panels show that the Galactic distances of TYC 5241-986-1 A are possibly consistent with several of the associations, but it lies on the periphery of the distributions in any case. As a supplement to the comparisons in the figure, we calculate the probability that TYC 5241-986-1 A is a member of one of the associations using the Bayesian analysis tools of Malo et al. (2013). We found the highest membership probability over our range of photometric distances is with the Columba association, although only 30 per cent at 65 pc (a distance inconsistent with TYC 5241-986-1 A being of similar age to Columba). Thus, without a measured parallax to better constrain the system’s distance, we cannot suggest any membership assignment to any of the individual associations and can only conclude that the TYC 5241-986-1 system’s kinematics and youth are consistent with other nearby young stars in the solar neighbourhood that comprise the Local Association.

4 MID-INFRARED EXCESS

4.1 Fidelity of the *WISE* data

In order to check the quality of the *WISE* $W4$ excess, we performed a number of checks. First, we examined the *WISE* images to ensure that the object appeared as a point-like source in all four bands (3.4, 4.6, 12, 22 μm). Next we checked the aperture magnitude in the $W4$ band. This was found to be 7.56 ± 0.32 , in good agreement with the point spread function (PSF) magnitude of 7.36 ± 0.18 . We then examined the individual measurements, we found that there were several anomalously bright detections in the catalogue for this source. As the source was flagged as having several measurements contaminated by scattered moonlight, we contacted the *WISE* helpdesk who informed us that the anomalous measurements had not been used in the final *WISE* co-add. Five images were used to produce the final $W4$ catalogue values for this star. In two of these it was detected at a significance of over 3σ , this makes a brief transient event unlikely as the cause for the excess. Additionally the source has a χ^2 goodness of fit statistic of 1.06 for the $W4$ band profile fit, further supporting the fidelity of the detection. Hence we assume that the excess in $W4$ is real and has an astrophysical cause.

4.2 *Herschel* observations

It is virtually impossible to characterize the excess based on only a single data point. Additionally, while we have exhaustively endeavoured to confirm the reliability of the *WISE* $W4$ excess, there is always the possibility of a spurious measurement for reasons we have not considered. Hence we obtained *Herschel*/Photodetecting Array Camera and Spectrometer (PACS) 70 and 160 μm observa-

We observed TYC 5241-986-1 A with the PACS photometer (Poglitsch et al. 2010) onboard *Herschel* (Pilbratt et al. 2010) on 2012 December 31. The observing strategy consisted of two consecutive PACS mini-scan maps (program ‘OT1_jolofsso_1’, OBSIDs 1342257974 and 1342257975) in the blue filter (70 μm). The observing duration was 2470 s per mini-scan map. When observing with PACS with the blue camera, data are also simultaneously acquired with the red camera (160 μm). The data were processed using the *Herschel* Interactive Processing Environment (HIPE, version 10.0.667), using standard scripts that include bad pixel flagging, detection and correction for glitches and HighPass filtering in order to remove the $1/f$ noise (see Poglitsch et al. 2010 for more details). Fig. 1 shows the PACS images at 70 and 160 μm . One can immediately notice the two close-by sources that are background galaxies. The primary, TYC 5241-986-1 A, is heavily contaminated by their emission at 160 μm , rendering any flux extraction impossible. We consequently only used the 70 μm observation in our analysis. Given the proximity of the background galaxy to our source of interest we used the IDL package *STARFINDER*⁴ to perform PSF photometry of the source. An empirical PSF of the Vesta asteroid, obtained on OD 160, with the same scan speed as our observations (20 arcsec s^{-1}), is used within *STARFINDER*. From this we detected a source at $22^{\text{h}}59^{\text{m}}35^{\text{s}}.23$, $-07^{\circ}02'24''.09$ (J2000) with a flux of 7.1 mJy in the 70 μm map. This is 2.6 arcsec from the predicted 2013.0 position of TYC 5241-986-1 A, comparable with the approximate *Herschel* positional error of 2.5 arcsec. To estimate the noise level and thus the quality of the detection, we randomly placed apertures on the 70 μm map. Because of a smaller detector coverage, map borders are noisier and not representative of the noise close to the source. Therefore the different apertures were placed within a distance of 80 pixels to the central pixel. We then extracted the aperture photometry for all of these apertures and fitted a Gaussian profile to the flux distribution histogram to estimate the σ uncertainty of 1.8 mJy for our source. Overall, the estimated uncertainty is consistent with predictions from the *HERSCHEL*.SPOT⁵ software.

4.3 Is the excess caused by a debris disc?

Mid-infrared excesses around stars older than ~ 10 Myr are characteristic of debris discs. Fig. 7 shows that there is a clear excess above the photosphere at $W4$ and 70 μm . To characterize the spectral energy distribution (SED), we fitted a series of Planck functions to the excess and computed the reduced χ^2 statistic for each. As shown in Fig. 7, the excess fits a temperature in the 100–175 K range with a best fit at 135 K. This equates to a typical distance of approximately 1.5 au from this type of star (equation 3 from Wyatt 2008). Smith et al. (2006) identified candidate debris discs around HD 95650 (M2) and BD +21°2486 (K5) both of which have excess at 70 μm but not at 24 μm . The excess in our source exists both at 22 and 70 μm , indicating that the candidate disc is more like the one proposed around the early M dwarf TWA 7, which has excess at 24 and 70 μm . Low et al. (2005) attribute this to an 80 K disc. Given TYC 5241-986-1 A is likely to be substantially older than the TW Hydrae association, it is likely that its disc has recently been replenished by some process. From these fits we estimate the dust mass to be $2.5 \times 10^{-5} M_{\oplus}$ using equation (5) from Wyatt (2008).

⁴ <http://www.bo.astro.it/StarFinder/paper6.htm>, Diolaiti et al. (2000).

⁵ <http://herschel.esac.esa.int/Tools.shtml> version 6.2.0.

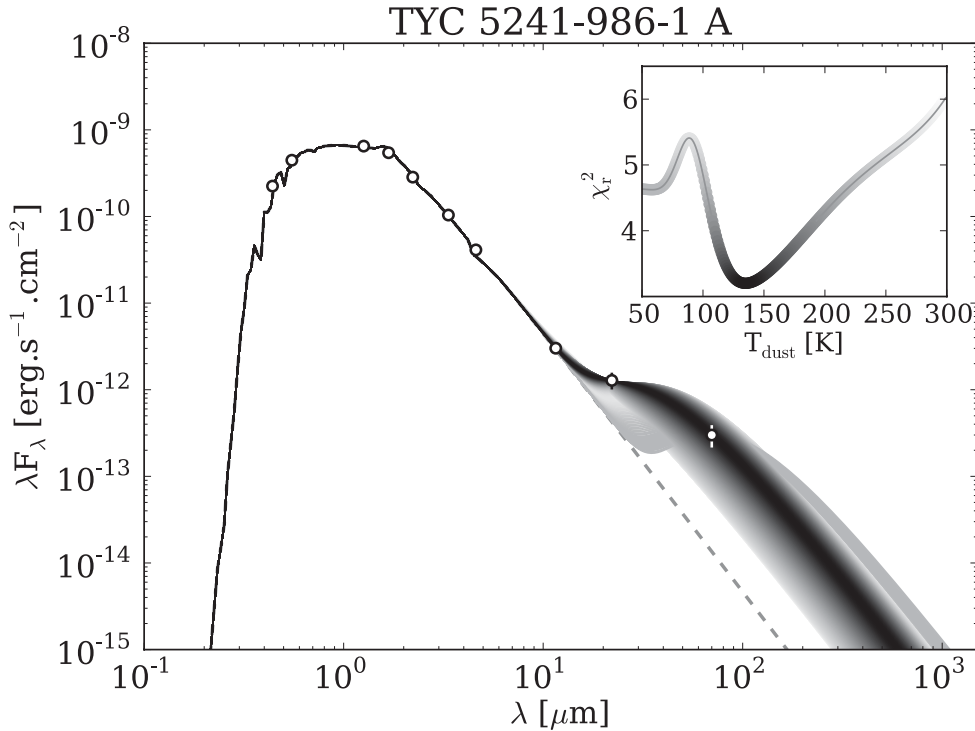


Figure 7. The SED of TYC 5241-986-1 A. The points are from left to right, Tycho *B* and *V* (Høg et al. 2000), 2MASS *J*, *H* and *K_s* (Skrutskie et al. 2006), *WISE* *W1*, *W2*, *W3* and *W4* (Wright et al. 2010; Cutri et al. 2012) and our *Herschel*/PACS 70 μm detection. The solid line is a fit to a 4200 K model of the photosphere from Castelli & Kurucz (2003). The plotted error bars represent 1σ confidence limits. A series of Planck functions with different temperatures were fitted to the excess and their reduced χ^2 goodness of fit statistic computed (see inset). The weight of the black and grey lines beyond 10 μm represents their goodness of fit (darker more likely). Note there are a number of fits with temperatures around 50 K with reasonable χ^2 values. However, these do not match the *W4* excess well. From this plot we characterize the emission as being caused by dust at approximately 100–175 K.

4.4 Is the excess caused by a background galaxy?

Caution must always be exercised when associating far-infrared detections with optical counterparts. This is starkly demonstrated by the case of TWA 13A. This was proposed to have a debris disc by Low et al. (2005) based on a single-band excess at 70 μm . However further examination by Plavchan et al. (2009) identified that the excess was caused by a background source (likely a galaxy) approximately 10 arcsec away. Our source differs from this case in two respects. First, we have an excess in both the *WISE* *W4* band and the *Herschel* 70 μm band. Secondly, our *Herschel* detection is within 3 arcsec of the expected position of the star, significantly closer than TWA 13A is to its 70 μm counterpart. In fact our object more closely resembles TWA 7.

Sibthorpe et al. (2012) use galaxy number counts from *Herschel* surveys to estimate the probability of a coincident background galaxy being associated with a source. To quantify the possibility of a chance alignment, we applied their formula to derive a probability of 0.048 per cent that a source of 7 mJy would fall within 3 arcsec of a particular position. It should be noted that our survey returned 38 candidate young stars with proper motions within 5σ of their proposed primaries. While only our star and TYC 7443-1102-1 B are obviously good candidates to be real companions, we multiply our 0.048 per cent by 38 to yield a coincident probability of 1.8 per cent for our study as a whole. As most of the 38 objects are clear background stars, this probability is likely to be artificially inflated. However, it should be noted that Sibthorpe et al. (2012)’s analysis assumes a random distribution of galaxies. As seen in Fig. 1 there are two galaxies within an arcminute of TYC 5241-986-1 A. One of these, SDSS J225934.58–070231.5 has a measured SDSS photo-

metric redshift of 0.25 ± 0.09 . The possible bias caused by galaxy clustering may increase the probability of a chance alignment.

We modelled the SED of this object as a combination of a late-K dwarf and a 100–175 K Planck function. To first order, a background extragalactic source must also match a 100–175 K Planck function. While the SED of a galaxy is complex, it is dominated at far-infrared wavelengths by emission from cold dust. Smith et al. (2012) studied *Herschel* selected galaxies in the local universe and found that the mean grey body temperature (which describes the dust) was 26.1 ± 3.5 K. This is substantially different from our best-fitting temperature of 100–175 K. This study quotes values for rest-frame wavelength SEDs so clearly redshift could alter the SED of the hypothetical background galaxy. However, redshift would gradually push the peak of the dust SED redward, making it an even poorer fit to a 100–175 K blackbody. It is possible that at redshifts of >2 the dust component for a typical galaxy will move beyond the *Herschel* 70 μm band. However this would make it unassociated with the low-redshift galaxies in close proximity to the star. In this case the probability of chance alignment would be that calculated for a random distribution of background galaxies. Our extremely conservative determination of a chance alignment to a background galaxy was previously calculated to be 1.8 per cent. In summary, while we cannot conclusively rule out a chance alignment with a background source, we determine this possibility to be highly unlikely.

5 CONCLUSIONS

We have identified a young hierarchical triple system. Spectroscopic observations of the primary indicate that it is an active, moderately

young (20 to ~ 125 Myr) late-K dwarf. From its radial velocity measurements, proper motions and photometric distance we associate the system with the Local Association, but cannot link it to any specific young moving group. Observations of the secondary and tertiary components indicate that these are a pair of active M 4.5 ± 0.5 dwarfs. From these spectral types we derived the total mass of the system and found it to be extremely loosely bound compared to field binaries. The primary has excess at *WISE* 24 μm and *Herschel*/PACS 70 μm . While we cannot completely rule out contamination by a background galaxy, we find it unlikely based on the SED of the excess and the likelihood of a chance alignment. We consider a debris disc with a temperatures between 100 and 175 K to be the most likely cause of the excess. Such debris discs around a stars of this apparent age and spectral type are extremely rare and this source is one of only a handful of candidate debris discs around late-type stars older than ~ 20 Myr.

ACKNOWLEDGEMENTS

We thank Sebastian Lépine for making his proper motion catalogue available for the production of the input catalogue. We also thank Tom Herbst for discussions on our paper draft, Wolfgang Brandner and Reinhard Mundt for their expertise on activity signatures in M dwarfs, Thomas Robitaille for helpful discussions, Chad Bender for the use of his spectral cross-correlation software and Elisabete Da Cunha for her mastery of galaxy SEDs. Thanks to Bruce Sibthorpe for making his background confusion script available. This publication makes use of data from MPIA director's discretionary time and we thank the staff at the MPG/ESO 2.2-m telescope in La Silla for undertaking our observations. We thank Calar Alto Observatory for allocation of director's discretionary time to this programme. This publication makes use of data products from the *Wide-field Infrared Survey Explorer*, which is a joint project of the University of California, Los Angeles, and the Jet Propulsion Laboratory/California Institute of Technology, funded by the National Aeronautics and Space Administration. We would especially like to thank Roc Cutri and the *WISE* helpdesk team for assisting us with questions about *WISE* data. This research has made use of data obtained from the SuperCOSMOS Science Archive, prepared and hosted by the Wide Field Astronomy Unit, Institute for Astronomy, University of Edinburgh, which is funded by the UK Science and Technology Facilities Council. *Herschel* is an ESA space observatory with science instruments provided by European-led Principal Investigator consortia and with important participation from NASA. The *Herschel* spacecraft was designed, built, tested and launched under a contract to ESA managed by the *Herschel/Planck* Project team by an industrial consortium under the overall responsibility of the prime contractor Thales Alenia Space (Cannes), and including Astrium (Friedrichshafen) responsible for the payload module and for system testing at spacecraft level, Thales Alenia Space (Turin) responsible for the service module and Astrium (Toulouse) responsible for the telescope, with in excess of a hundred subcontractors. This research has made use of the SIMBAD database, operated at CDS, Strasbourg, France and data products from the Two Micron All Sky Survey, which is a joint project of the University of Massachusetts and the Infrared Processing and Analysis Center/California Institute of Technology, funded by the National Aeronautics and Space Administration and the National Science Foundation. Funding for the SDSS and SDSS-II has been provided by the Alfred P. Sloan Foundation, the Participating Institutions, the National Science Foundation, the US Department of Energy, the National Aeronautics and Space Admin-

istration, the Japanese Monbukagakusho, the Max Planck Society and the Higher Education Funding Council for England. The SDSS Web Site is <http://www.sdss.org/>. The SDSS is managed by the Astrophysical Research Consortium for the Participating Institutions. The Participating Institutions are the American Museum of Natural History, Astrophysical Institute Potsdam, University of Basel, University of Cambridge, Case Western Reserve University, University of Chicago, Drexel University, Fermilab, the Institute for Advanced Study, the Japan Participation Group, Johns Hopkins University, the Joint Institute for Nuclear Astrophysics, the Kavli Institute for Particle Astrophysics and Cosmology, the Korean Scientist Group, the Chinese Academy of Sciences (LAMOST), Los Alamos National Laboratory, the Max-Planck-Institute for Astronomy (MPIA), the Max-Planck-Institute for Astrophysics (MPA), New Mexico State University, Ohio State University, University of Pittsburgh, University of Portsmouth, Princeton University, the United States Naval Observatory and the University of Washington.

REFERENCES

- Ahn C. P. et al., 2012, *ApJS*, 203, 21
 Avenhaus H., Schmid H. M., Meyer M. R., 2012, *A&A*, 548, A105
 Backman D. E., Paresce F., 1993, in Levy E. H., Lunine J. I., eds, *Protostars and Planets III*. University of Arizona Press, Tucson, p. 1253
 Baraffe I., Chabrier G., Allard F., Hauschildt P. H., 1998, *A&A*, 337, 403
 Barenfeld S. A., Bubar E. J., Mamajek E. E., Young P. A., 2013, *ApJ*, 766, 6
 Castelli F., Kurucz R. L., 2003, in Piskunov N., Weiss W. W., Gray D. F., eds, *Proc. IAU Symp. 210, Modelling of Stellar Atmospheres*. Astron. Soc. Pac., San Francisco, p. 20
 Close L. M., Siegler N., Freed M., Biller B., 2003, *ApJ*, 587, 407
 Currie T., Kenyon S. J., Balog Z., Rieke G., Bragg A., Bromley B., 2008, *ApJ*, 672, 558
 Cutri R. M. et al., 2012, *Explanatory Supplement to the WISE All-Sky Data Release Products*
 Delgado-Donate E. J., Clarke C. J., Bate M. R., Hodgkin S. T., 2004, *MNRAS*, 351, 617
 Dhital S., West A. A., Stassun K. G., Law N. M., 2013, *Astron. Nachr.*, 334, 14
 Diolaiti E., Bendinelli O., Bonaccini D., Close L., Currie D., Parmeggiani G., 2000, *A&AS*, 147, 335
 Donaldson J. K. et al., 2012, *ApJ*, 753, 147
 Dupuy T. J., Liu M. C., 2012, *ApJS*, 201, 19
 Eiroa C. et al., 2013, *A&A*, 518, 131
 Eyer L., Blake C., 2005, *MNRAS*, 358, 30
 Fischer D. A., Marcy G. W., 1992, *ApJ*, 396, 178
 Forbrich J., Lada C. J., Muench A. A., Teixeira P. S., 2008, *ApJ*, 687, 1107
 Fujiwara H. et al., 2013, *A&A*, 550, A45
 Hall J. C., 1996, *PASP*, 108, 313
 Hambly N. et al., 2001, *MNRAS*, 326, 1279
 Heng K., Malik M., 2013, *MNRAS*, 432, 2562
 Høg E. et al., 2000, *A&A*, 355, L27
 Houdebine E. R., Doyle J. G., Koscielicki M., 1995, *A&A*, 294, 773
 Hynes R. I., 2002, *A&A*, 382, 752
 Johnson D. R. H., Soderblom D. R., 1987, *AJ*, 93, 864
 Kaczmarek T., Olczak C., Pfalzner S., 2011, *A&A*, 528, A144
 Kalas P., Liu M. C., Matthews B. C., 2004, *Sci*, 303, 1990
 Kaufer A., Stahl O., Tubbesing S., Nørregaard P., Avila G., Francois P., Pasquini L., Pizzella A., 1999, *Messenger*, 95, 8
 Kenyon S. J., Hartmann L., 1995, *ApJS*, 101, 117
 King J. R., Villareal A. R., Soderblom D. R., Gulliver A. F., Adelman S. J., 2003, *AJ*, 125, 1980
 King R. R., Goodwin S. P., Parker R. J., Patience J., 2013, *MNRAS*, 427, 2636
 Kouwenhoven M. B. N., Goodwin S. P., Parker R. J., Davies M. B., Malmberg D., Kroupa P., 2010, *MNRAS*, 404, 1835

- Lépine S., Bongiorno B., 2007, *AJ*, 133, 889
 Lépine S., Shara M. M., 2005, *AJ*, 129, 1483
 Lépine S., Simon M., 2009, *AJ*, 137, 3632
 Lépine S., Rich R. M., Shara M. M., 2003, *AJ*, 125, 1598
 Lestrade J.-F., Wyatt M. C., Bertoldi F., Dent W. R. F., Menten K. M., 2006, *A&A*, 460, 733
 Lestrade J.-F., Wyatt M. C., Bertoldi F., Menten K. M., Labaigt G., 2009, *A&A*, 506, 1455
 Lestrade J.-F. et al., 2012, *A&A*, 548, A86
 Liu M. C., Matthews B. C., Williams J. P., Kalas P. G., 2004, *ApJ*, 608, 526
 López-Santiago J., Montes D., Gálvez-Ortiz M. C., Crespo-Chacón I., Martínez-Arnáiz R. M., Fernández-Figueroa M. J., de Castro E., Cornide M., 2010, *A&A*, 514, A97
 Low F. J., Smith P. S., Werner M., Chen C., Krause V., Jura M., Hines D. C., 2005, *ApJ*, 631, 1170
 Malo L., Doyon R., Lafrenière D., Artigau E., Gagné J., Baron F., Riedel A., 2013, *ApJ*, 762, 88
 Mamajek E. E., Feigelson E. D., 2001, in Jayawardhana R., Greene T., eds, *ASP Conf. Ser. Vol. 244, Young Stars Near Earth: Progress and Prospects*. Astron. Soc. Pac., San Francisco, p. 104
 Mamajek E. E., Hillenbrand L. A., 2008, *ApJ*, 687, 1264
 Mannings V., Barlow M. J., 1998, *ApJ*, 497, 330
 Martin D. C. et al., 2005, *ApJ*, 619, L1
 Mauas P. J. D., 2000, *ApJ*, 539, 858
 Mentuch E., Brandeker A., van Kerkwijk M. H., Jayawardhana R., Hauschildt P. H., 2008, *ApJ*, 689, 1127
 Moór A. et al., 2011, *ApJS*, 193, 4
 Oke J. B., 1990, *AJ*, 99, 1621
 Pilbratt G. L. et al., 2010, *A&A*, 518, L1
 Plavchan P., Werner M. W., Chen C. H., Stapelfeldt K. R., Su K. Y. L., Stauffer J. R., Song I., 2009, *ApJ*, 698, 1068
 Poglitsch A. et al., 2010, *A&A*, 518, L2
 Prato L., Simon M., Mazeh T., McLean I. S., Norman D., Zucker S., 2002, *ApJ*, 569, 863
 Reid I. N., Gizis J. E., 1997, *AJ*, 113, 2246
 Reipurth B., Mikkola S., 2012, *Nat*, 492, 221
 Schlieder J. E., Lépine S., Simon M., 2012a, *AJ*, 143, 80
 Schlieder J. E., Lépine S., Rice E., Simon M., Fielding D., Tomasino R., 2012b, *AJ*, 143, 114
 Schmitt J. H. M. M., Fleming T. A., Giampapa M. S., 1995, *ApJ*, 450, 392
 Shkolnik E. L., Liu M. C., Reid I. N., Dupuy T., Weinberger A. J., 2011, *ApJ*, 727, 6
 Shkolnik E. L., Anglada-Escudé G., Liu M. C., Bowler B. P., Weinberger A. J., Boss A. P., Reid I. N., Tamura M., 2012, *ApJ*, 758, 56
 Sibthorpe B., Ivison R. J., Massey R. J., Roseboom I. G., van der Werf P. P., Matthews B. C., Greaves J. S., 2012, *MNRAS*, 428, L6
 Simon M., Schlieder J. E., Constantin A.-M., Silverstein M., 2012, *ApJ*, 751, 114
 Skinner C., Barlow M., Justtanont K., 1992, *MNRAS*, 255, 31
 Skrutskie M. F. et al., 2006, *AJ*, 131, 1163
 Smith P. S., Hines D. C., Low F. J., Gehrz R. D., Polomski E. F., Woodward C. E., 2006, *ApJ*, 644, L125
 Smith D. J. B. et al., 2012, *MNRAS*, 427, 703
 Soderblom D. R., Mayor M., 1993, *AJ*, 105, 226
 Stauffer J. R., Schultz G., Kirkpatrick J. D., 1998, *ApJ*, 499, L199
 Su K. Y. L. et al., 2006, *ApJ*, 653, 675
 Torres C. A. O., Quast G. R., Melo C. H. F., Sterzik M. F., 2008, in Reipurth B., ed., *ASP Monograph Publications, Vol. 5, Handbook of Star Forming Regions, Vol. II, The Southern Sky*. Astron. Soc. Pac., San Francisco, p. 757
 Trilling D. E. et al., 2008, *ApJ*, 674, 1086
 Voges W. et al., 2000, *IAU Circ.*, 7432, 3
 West A. A., Hawley S. L., Bochanski J. J., Covey K. R., Reid I. N., Dhital S., Hilton E. J., Masuda M., 2008, *AJ*, 135, 785
 Worden S. P., Schneeberger T. J., Giampapa M. S., 1981, *ApJS*, 46, 159
 Wright E. L. et al., 2010, *AJ*, 140, 1868
 Wyatt M. C., 2008, *ARA&A*, 46, 339
 Wyatt M. C. et al., 2012, *MNRAS*, 424, 1206
 Zuckerman B., Song I., 2004, *ARA&A*, 42, 685

This paper has been typeset from a $\text{\TeX}/\text{\LaTeX}$ file prepared by the author.